

Analyst

Accepted Manuscript



This is an *Accepted Manuscript*, which has been through the Royal Society of Chemistry peer review process and has been accepted for publication.

Accepted Manuscripts are published online shortly after acceptance, before technical editing, formatting and proof reading. Using this free service, authors can make their results available to the community, in citable form, before we publish the edited article. We will replace this *Accepted Manuscript* with the edited and formatted *Advance Article* as soon as it is available.

You can find more information about *Accepted Manuscripts* in the [Information for Authors](#).

Please note that technical editing may introduce minor changes to the text and/or graphics, which may alter content. The journal's standard [Terms & Conditions](#) and the [Ethical guidelines](#) still apply. In no event shall the Royal Society of Chemistry be held responsible for any errors or omissions in this *Accepted Manuscript* or any consequences arising from the use of any information it contains.

Real-time monitoring of H₂O₂ release from single cells using nanoporous gold microelectrodes decorated with platinum nanoparticles

Cite this: DOI: 10.1039/x0xx00000x

Chong Xiao, Yan-Ling Liu, Jia-Quan Xu, Song-Wei Lv, Shan Guo and Wei-Hua Huang*

Received 00th,
Accepted 00th

DOI: 10.1039/x0xx00000x

www.rsc.org/

Here we report a self-supported nanoporous gold microelectrode decorated with well-dispersed and tiny platinum nanoparticles as an electrochemical nonenzymatic hydrogen peroxide biosensor. Nanoporous gold was fabricated by electrochemical alloying/dealloying and then small-sized platinum nanoparticles were electrodeposited uniformly thereon. The novel hybrid nanostructure endows the sensor with high sensitivity and selectivity towards the reduction of hydrogen peroxide with a low detection limit of 0.3 nM. The sensor has been successfully applied to the measurement of H₂O₂ release from single isolated human breast cancer cell, demonstrating its great potential for further physiological and pathological applications.

1. Introduction

Hydrogen peroxide (H₂O₂), as a signaling molecule, plays critical roles in regulating diverse biological processes,¹ such as DNA repair,² oxidative activity,³ host defense,⁴ and apoptosis.⁵ Thus, rapid, accurate and sensitive determination of H₂O₂ is of great importance to study its physiological and pathological functions. Techniques available mainly include titrimetry,⁶ spectrophotometry,⁷ chemiluminescence,⁸ electrochemistry,⁹⁻¹¹ fluorescence¹² and electron spin resonance.¹³ Among them, electrochemical sensor, especially based on microelectrodes, is distinguished for its unique characteristics of high sensitivity, fast response and easy miniaturization, which enable it to be a powerful tool for real-time quantitative detection in biological systems.^{14,15}

A number of electrochemical enzyme sensors have been developed to improve the electrocatalysis to H₂O₂.^{9,16,17} Nevertheless, the biocatalytic activities of enzymes are easily affected by the environment (such as temperature and pH) and the immobilization procedure, and the detection limits are

usually restricted within the sub-micromolar regime. Subsequently, the advent of nanomaterials including metal nanoparticles,¹⁸ carbon nanomaterials^{19,20} and metallic oxide nanostructures,²¹ brought H₂O₂ sensing to non-enzymatic era, and tremendous sensors with high sensitivity and good stability have been constructed. Many biosensors with good responsiveness have been developed and used for measurement of H₂O₂ released from populations of living cells or the concentrated cytoplasm after lysis.²²⁻²⁶ Notably, platinum (Pt) nanomaterials act as an excellent electrochemical catalyst to H₂O₂, benefiting from its function in promoting the electron transfer and reducing the over-potential.¹¹ In the field of single cell analysis using Pt nanomaterials as the catalyst, pioneering work of H₂O₂ monitoring from single isolated cell was reported by Amatore' group to study oxidative stress using platinized carbon-fiber microelectrode.^{14,27} And our group developed uniform Pt nanoparticles (NPs) modified carbon fiber microelectrode and monitored the oxidative burst from individual living plant protoplasts.²⁸

To increase Pt loading and obtain uniformly small-sized NPs, carbon nanotubes,²⁹ graphene,³⁰ nanowires³¹ and polymer³² have been explored as templates to disperse PtNPs homogeneously on the electrode surface. However, the area enhancement is limited because it focuses only on the utilization of the geometric surface. Furthermore, the composite nanostructures usually need to be further modified onto the surface of the electrodes. The assembled electrochemical sensor usually exhibit an undesirably low electronic conductance as a consequence of exceptionally low electron transport in the nanomaterials as well as the high contact resistances between the current collector and electrodes.³³⁻³⁵ So far, there are

Key Laboratory of Analytical Chemistry for Biology and Medicine (Ministry of Education), College of Chemistry and Molecular Sciences, Wuhan University, Wuhan, 430072, China. E-mail: whhuang@whu.edu.cn; Fax: +86-27-68754067; Tel: +86-27-68752149

Electronic supplementary information (ESI) available: Fig. S1-Fig. S6, see DOI:10.1039/b000000x/

few reports concerning three dimensional (3D) and conductive substrate to support nanoparticles for sensors construction.

Herein, we report a self-supported microelectrode with a seamless solid/nanoporous gold/PtNPs hybrid (NPG/PtNPs) nanostructure to develop H_2O_2 biosensor with high sensitivity, as well as high spatial and temporal resolution. Gold microwire structured with bicontinuous nanoporous, which was fabricated by electrochemical alloying/dealloying in an electrolyte composed of ZnCl_2 and benzyl alcohol (BA),³⁵⁻³⁸ was adopted as self-supported microelectrodes to adequately make use of the surface area of 3D nanomaterials. Then small-sized and uniform PtNPs were electrodeposited on the ligament of mercaptoethylamine-pretreated NPG. The as-prepared nanostructure exhibits remarkable catalytic activity toward electrochemical reduction of H_2O_2 with a sub-nanomolar sensitivity. The excellent performance results from the elaborate design that NPG provides interconnected nanoporous channels to facilitate the transports of H_2O_2 and electron, and the continuous skeletons offer large area for PtNPs loading and avoid the particle aggregation. Moreover direct generation of 3D bicontinuous NPG layer on the gold microwires could minimize the contact resistances among current collector of solid gold wire, nanoporous gold skeleton and PtNPs. The sensor was further successfully used for real-time monitoring of H_2O_2 released from single human breast cancer cells.

2. Experimental

2.1 Reagents

Gold wire (25 μm in diameter, 99.99+% purity) was purchased from Goodfellow Cambridge Limited. Phobol myristate acetate (PMA), chloroplatinic acid hexahydrate ($\text{H}_2\text{PtCl}_6 \cdot 6\text{H}_2\text{O}$), catalase, 3-morpholinopyridone (SIN-1) and KO_2 were purchased from Sigma-Aldrich. Cysteamine hydrochloride ($\text{C}_2\text{H}_7\text{NS} \cdot \text{HCl}$) was obtained from Alfa Aesar. Hydrogen peroxide (H_2O_2 , 30%), zinc chloride (ZnCl_2), concentrated H_2SO_4 , benzyl alcohol (BA) were of analytical grade and obtained from Sinopharm Chemical Reagent Co., Ltd. Solutions with desired concentration of H_2O_2 were freshly diluted with deoxygenized 0.1 M phosphate buffer solution (PBS, pH 7.4) from the 30% solution. In the selectivity test, superoxide anion ($\text{O}_2^{\cdot -}$) was derived from dissolved KO_2 in the DMSO solution, ONOO^- was generated by dissolving 3-morpholinopyridone (SIN-1) into PBS (pH 7.4), and hypochlorite anion (ClO^-) was generated by NaClO . For all the experiments, deionized water (18.0 M Ω) purified by a Millipore system was used.

2.2 Apparatus

All electrochemical measurements were carried out on a CHI 660A electrochemical workstation (CHI Instruments, Shanghai, China) at room temperature. A three-electrode system was used in the experiment including a NPG/PtNPs working electrode (WE), Ag/AgCl reference electrode and Pt counter electrode. And two-electrode system was employed for the cell experiments. SEM images were obtained on a field-emission scanning electron microscope (Zeiss SIGMA). The TEM images were acquired on a

JEM-2100 transmission electron microscope. In cell experiment, two micromanipulators (TransferMan NK2, Eppendorf, Hamburg, Germany) were used for precise positioning. A TS2-60 multi Syringe pump (LongerPump Co., Ltd) was in conjunction with one of the micromanipulators for stimulant injection. An inverted fluorescent microscope (Axiovert 200M, Zeiss, Germany) was utilized for observation.

2.3 Fabrication of NPG microelectrode

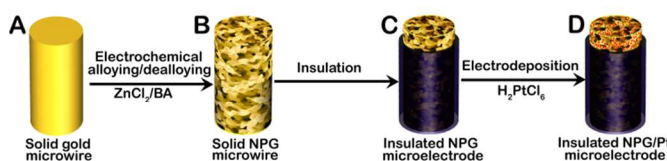
In brief, gold microwire (Scheme 1A) was cut into 0.3 cm in length, then was connected to a copper wire via conductive glue and the joint was wrapped with tape, followed by seal with polydimethylsiloxane. Before alloying/dealloying, the gold wires were degreased ultrasonically in acetone, ethanol and distilled water for a few minutes, respectively. The electrochemical alloying/dealloying process was performed in a three-electrode electrochemical cell, in which Zn plate and Zn wire were used as the auxiliary electrode and the reference electrode in a BA electrolyte containing 1.5 M ZnCl_2 . 3D bicontinuous nanoporous layer was generated on polished gold wires after 5 cycles in the potential range from -0.72 to 1.88 V at 120°C with a scan rate of 10 mV/s (Scheme 1B).³⁵⁻³⁸ Before and after etch, the electrode was cleaned by cyclic voltammetry in 0.5 M H_2SO_4 from 0.4 V to 1.5 V until a reproducible scan was obtained. The NPG electrode was thoroughly rinsed with deionized water and dried under flowing nitrogen.

2.4 Electrodeposition of PtNPs into NPG

To enhance the signal/noise of NPG for amperometric detection on single cells, we obtained a NPG microdisk electrode by selectively insulating the electrode with photoresist that has been described in our previous work.³⁹ Briefly, the microelectrode was immersed into the AZ4620 photoresist for 5 minutes, followed by heating in the oven at 75°C for 4 minutes and 105°C for 6 minutes. The above process was repeated again to ensure all of the active area was insulated with photoresist. The precise removal of photoresist covered on the tip of the electrode was performed in $\text{H}_2\text{SO}_4/\text{H}_2\text{O}_2$ (v/v=7:3) solution with the aid of a micromanipulator, revealing the exposed tip 1-2 μm in length (Scheme 1C). Before the electrodeposition of PtNPs, the clean NPG microdisk electrode was immersed in 0.1 mM mercaptoethylamine or cysteamine (Cys) solution for 4 h at room temperature to form a NPG-Cys self-assembly microelectrode. At the end of this period, the microdisk electrode (NPG-Cys) was rinsed with double distilled water to wash off the physically adsorbed mercaptoethylamine. After standing in 0.5 mM H_2PtCl_6 solution for 2 hours, the NPG-Cys microelectrode acted as the WE to electrodeposit PtNPs for 100 s at the potential of -0.6 V (vs Ag/AgCl) with 0.2 M Na_2SO_4 as supporting electrolyte (Scheme 1D).

2.5 Single cell experiments

Human breast cancer cells MCF-7 were obtained from China Center for Type Culture Collection. The cells were maintained in Dulbecco's modified eagle medium supplemented with 10% fetal bovine serum, 1% double-antibody and incubated at 37°C in a



Scheme 1. The fabrication of hybrid microelectrodes. (A) Solid gold microwire. (B) 3D bicontinuous NPG layer is formed directly on the solid gold microwire by electrochemical alloying/dealloying in a mixed electrolyte of BA and ZnCl₂. (C) The insulated NPG microelectrode. (D) PtNPs are decorated onto nanopore channels of NPG microelectrode by electrodeposition in a mixed solution containing H₂PtCl₆.

humidified incubator (5% CO₂–95% air). Before cell experiments, the cells were transferred onto a slide to incubate for 24 h. Single cell experiments were performed at room temperature on the stage of the inverted fluorescent microscope placed in a copper shield. H₂O₂ released from single cells was real-time detected by the CHI 660A workstation at a constant potential of -0.2 V. For the detection of extracellular H₂O₂ released from MCF-7, the cells were stimulated with 100 ng/ml PMA.^{40,41} In control experiment, the cells were stimulated by PBS, or the cells were incubated with catalase for 10 min before stimulation by PMA.

3. Results and discussion

3.1 Fabrication and characterization of NPG/PtNPs

The fabrication process of NPG/PtNPs electrode was illustrated in Scheme 1. First, a 3D bicontinuous NPG layer was formed directly on the solid gold microwire by in situ electrochemical alloying/dealloying in a mixed electrolyte of ZnCl₂ and BA. Fig. 1A shows the representative top-view FESEM and TEM images of the NPG. A uniform and 3D bicontinuous porous structure can be clearly observed. Both gold skeletons and the pores are spatially interconnected, and the entire surfaces of NPG skeletons are smooth with a clear surface contour. Roughness factor was defined as the ratio between the real surface area and the geometrical area of electrode. In the case of the gold electrode, the charge associated with the reduction of gold oxide was proportional to the real active surface area of gold electrode.⁴² Cyclic voltammograms (CV) in 0.5

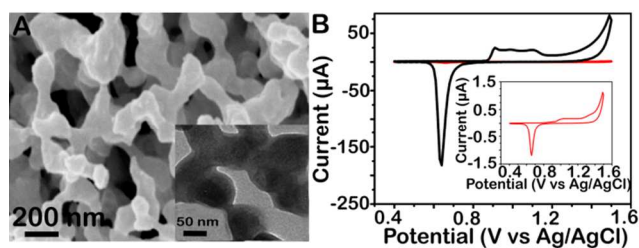


Fig. 1 (A) Top-view FESEM image of NPG, and the inset is TEM image of as-prepared NPG. (B) CV curves of gold microwire (red line) and NPG (black line) electrodes in 0.5 M H₂SO₄ solution at a scan rate of 100 mV/s. Inset: an enlarged curve for solid gold microwire.

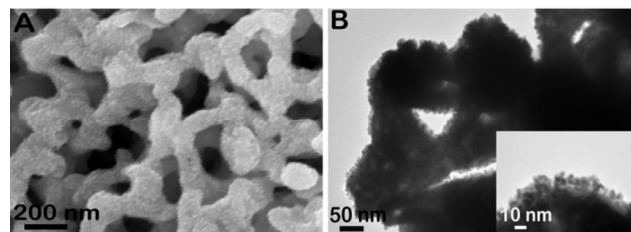


Fig. 2 (A) Top-view FESEM image of as-prepared NPG/PtNPs hybrid. (B) TEM image of as-prepared NPG/PtNPs hybrid.

M H₂SO₄ solution was employed to evaluate the electrochemically active surface area of the initial gold microwire and NPG (Fig. 1B), and the roughness factors of three individual NPG microelectrode were estimated to be 86, 110 and 115 respectively.

The NPG/PtNPs hybrid microelectrodes are synthesized by the electrodeposition with H₂PtCl₆ as the precursor. To obtain well-distributed PtNPs, here we modified the NPG microelectrode with a monolayer mercaptoethylamine through Au-S bond before electrodeposition, considering that the positive charged -NH₂ may promote the pre-absorption of PtCl₆²⁻ on the skeleton surface. The following results also confirmed that mercaptoethylamine layer on NPG could not only dramatically improve the Pt electrodeposition efficiency but also benefit the uniform dispersion of PtNPs, wherein the loading amount and morphology of PtNPs can be tailored by the H₂PtCl₆ concentration (Fig. S1), the applied potential (Fig. S2) and the electrodeposition time (Fig. S3), respectively. As illustrated in Fig. S2, the generated PtNPs become more dispersed when the potential is more negative. And at a constant potential of -0.6 V, the loading amount of PtNPs increases with the increasing concentration of H₂PtCl₆. In 0.1 mM H₂PtCl₆, only a few PtNPs can be observed from FESEM image; while the concentration increased to 1 mM, PtNPs start to aggregate, which lead to the blocking of nanopores on the gold skeleton. In the mixed solution containing 0.5 mM H₂PtCl₆, the small-sized PtNPs uniformly and directly grow into nanopores along the gold ligaments of the NPG at a constant applied potential of -0.6 V for 100 s. By contrast, under the same conditions, PtNPs aggregate seriously on the surface of the solid gold wire electrode (Fig. S3D). In Fig. 2A, the FESEM image reveals that there are lots of tiny PtNPs densely covered on the surface of the 3D bicontinuous NPG, forming a rough gold skeleton. Further from TEM image (Fig 2B), we can clearly see that PtNPs are well-dispersed with diameter of about 5–10 nm. The results indicate that the NPG used here as a supporting matrix could disperse PtNPs well, preventing them from serious aggregation and thus preserving the high catalytic performance of PtNPs. The unique bicontinuous structure of NPG and well-dispersed PtNPs will contribute to a large specific surface area of electrode/electrolyte interface, facilitating the enhanced electrocatalysis of NPG/PtNPs hybrid towards H₂O₂.

3.2 Electrochemical characterization of NPG/PtNPs

To eliminate individual difference of electrochemical behavior between different electrodes, the comparison between the NPG electrode and the NPG/PtNPs electrode was based on the same gold electrode. Recent studies found that performance of the H₂O₂ sensor

depends strongly on the size, distribution and loading amount of PtNPs on the electrode. The uniformly small-sized PtNPs could provide large number of active sites to contact H_2O_2 for the electrocatalytic process.^{29,43,44} Positive shift in the reduction peak potential and increase in the peak current were also obtained while increasing the loading of PtNPs on the electrode surface (Fig S4). At optimized conditions, it is clearly indicated that the reduction current of NPG/PtNPs microelectrode to H_2O_2 is much higher than that on NPG microelectrode (Fig. 3A). The onset reduction potential of the NPG/PtNPs microelectrode towards H_2O_2 was about -0.05 V, which is about 200 mV positively shifted compared with that of bare NPG electrode, and a reductive peak appeared at around -0.2 V. As a comparison, there is no apparent reduction current without H_2O_2 , further confirming that the current is generated via catalytic reduction of H_2O_2 . The positively shifted reduction potential and the significantly enhanced peak current clearly demonstrate that the NPG/PtNPs microelectrode has much higher catalysis towards the reduction of H_2O_2 than bare NPG microelectrode. This remarkable catalytic activity toward electrochemical reduction of H_2O_2 could be ascribed to the following factors. First, small-sized PtNPs intrinsically possess an excellent electrochemical catalysis to H_2O_2 . Second, a mercaptoethylamine modified 3D conductive NPG substrate which possessed much higher roughness and better electron transport was adopted as self-supported microelectrodes to support PtNPs. The structure could disperse and increase the load amount of small-sized PtNPs to provide large number of active sites, preventing them from aggregation. Third, synergistic electrocatalytic activity between the gold skeleton and PtNPs also plays an important role.

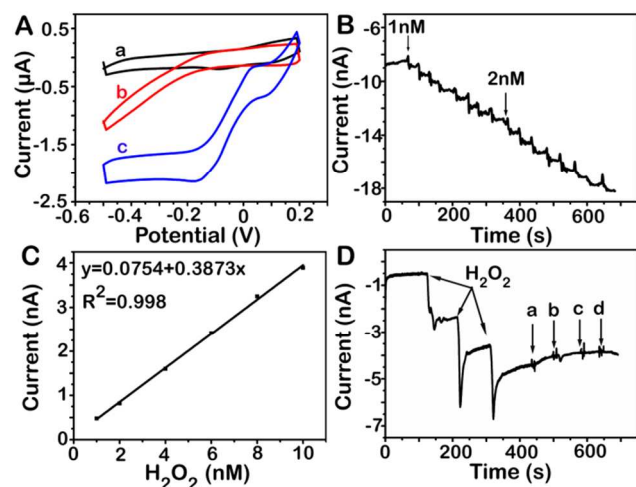


Fig. 3 (A) CV curves of NPG (b) and NPG/PtNPs (a, c) in deoxygenized PBS with 2 mM H_2O_2 (b, c) or without H_2O_2 (a) at a scan rate of 50 mV/s. (B) Amperometric responses of insulated NPG/PtNPs microelectrodes to the successive addition of H_2O_2 in 0.1 M PBS at an applied potential of -0.2 V. (C) Calibration curve of insulated NPG/PtNPs microelectrode for increasing concentration of H_2O_2 . (D) Amperometric responses of insulated NPG/PtNPs microelectrodes to the additions of 5 μM H_2O_2 , NO_2^- (a), ClO^- (b), ONOO^- (c) and O_2^- (d) respectively.

In order to further enhance signal/noise of NPG/PtNPs microelectrode for amperometric detection and the single cell experiments, the NPG/PtNPs microelectrode was insulated by photoresist and the tip was then selectively revealed to get a microdisk electrode (Scheme 1). Fig. 3B and Fig. S5 display steady-state amperometric responses of the NPG/PtNPs and solid gold/PtNPs microdisk electrodes with the same geometric size to different concentrations of H_2O_2 at a potential of -0.2 V. With additions of low concentrations of H_2O_2 (1 nM, 2 nM and 5 nM), there were no amperometric responses on the solid gold/PtNPs microdisk electrode, while the NPG/PtNPs microelectrode responded rapidly to achieve the maximum steady-state current within 5 s. An obvious step increase of the current could be observed when the concentration of H_2O_2 was as low as 1 nM. The detection limit of NPG/PtNPs microdisk electrode was calculated to be about 0.3 nM ($S/N = 3$), being the lowest of those reported previously as we known. The low detection limit of the sensor combined with its ultra-small geometric size facilitate NPG/PtNPs microdisk electrode to monitor H_2O_2 information on the single cell level or other biological microenvironments in real-time.

The selectivity of NPG/PtNPs toward H_2O_2 was further studied by investigation interfering species. In this work, the applied potential (-0.2 V) could minimize the responses of common interference species. The response of common coexisting reactive oxygen species (ROS) and compounds in biological system such as O_2^- , ONOO^- , ClO^- , NO_2^- , AA and UA was recorded at the NPG/PtNPs microdisk electrode. Fig. 3D and Fig. S6 showed that the response current of the sensor changed greatly after the addition of H_2O_2 , while nearly no current change could be observed with the addition of common ROS and compounds. This suggests the biosensor performs with high selectivity toward H_2O_2 over these biological relevant ROS and compounds.

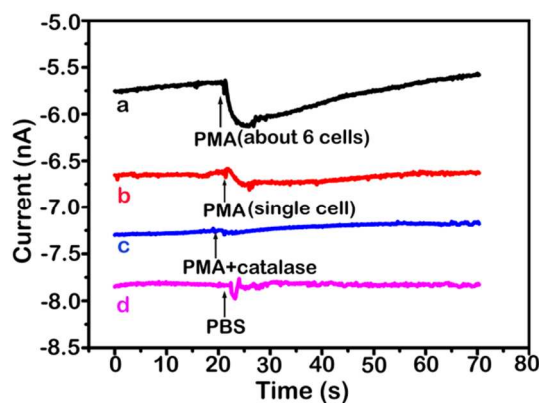


Fig. 4 Amperometric measurement of H_2O_2 released from MCF-7 cells at NPG/PtNPs microelectrodes. Typical responses of H_2O_2 release from about 6 MCF-7 cells (a) and a single MCF-7 cell (b) stimulated with PMA. Typical response of H_2O_2 release from MCF-7 cells stimulated with PMA after incubation of the cells with catalase (c). Typical response of H_2O_2 release from MCF-7 cells stimulated with PBS (d).

3.3 Monitoring of extracellular H₂O₂ released from single cells

It is of great significance to sensitively detect H₂O₂ owing to its diverse biological functions. Here, we used the constructed NPG/PtNPs microdisk electrode to monitor extracellular H₂O₂ released from single isolated MCF-7 cells. Before measurements, a slide with cells on it was placed in a chamber which served as an electrolytic cell. Under the microscope, we placed the sensor's tip 1 μm away from single MCF-7 cells' surface by a micromanipulator. In the opposite direction, a microcapillary filled with stimulus was positioned by another micromanipulator (this micromanipulator was connected with the pump for injection) to the place where the distance between the cell and the outlet of the microcapillary was about 70 μm. The H₂O₂ release was triggered by stimulation with 100 ng/mL phorbol myristate acetate (PMA) for 5 s, a compound that can induce H₂O₂ generation in cells.^{40,41} From Fig. 4 we can see that upon the injection of PMA, a sharp increase in current could be achieved within 5 s. Afterward, the current decreased to background level within 40 s, indicating that H₂O₂ is either consumed or diffused away from the electrode surface. Control experiments were carried out to confirm that the changes in the measured current observed were due to the electroreduction of H₂O₂ released from MCF-7 cells. In control experiment, the cells were stimulated by phosphate buffer, or the cells were incubated with catalase (with final concentration of 100 U/ml), a H₂O₂ scavenger, for 10 min before it was stimulated by PMA. No current increase was observed if catalase was added into PBS solution (Fig. 4). It indicated that the most of H₂O₂ molecule released from cells had been consumed by catalase. Similarly, no increase in current was observed when sham stimulus phosphate buffer was injected. The overall experimental results demonstrated the powerful ability of NPG/PtNPs microdisk electrode to detect H₂O₂ released from single MCF-7 cells with high sensitivity.

Conclusions

In summary, we have constructed a highly sensitive and selective H₂O₂ microsensor by electrodeposition small-sized and well-dispersed Pt nanoparticles on self-supported bicontinuous nanoporous gold microelectrodes. The microsensor displayed excellent electrocatalysis to the reduction of H₂O₂ and have a low detection limit of 0.3 nM. Owing to its ultra-small geometric size and high sensitivity, real-time monitoring of H₂O₂ release from single MCF-7 cell was achieved using this microsensor. The excellent catalytic performance and capacity to detect H₂O₂ on single cell level make this biosensor to be a potentially useful tool in the further physiological and pathological applications.

Acknowledgements

This work was supported by the National Science Foundation of China (Nos. 21375099, 91017013), Specialized Research Fund for the Doctoral Program of Higher Education (20120141110031) and the Fundamental Research Funds for the Central Universities (2042014kf0192).

References

1. T. Finkel and N. J. Holbrook, *Nature*, 2000, **408**, 239-247.
2. M. B. Yaffe and L. C. Cantley, *Nature*, 1999, **402**, 30-31.
3. J. D. Scott and T. Pawson, *Science*, 2009, **326**, 1220-1224.
4. D. Trachootham, J. Alexandre and P. Huang, *Nat. Rev. Drug Discov.*, 2009, **8**, 579-591.
5. M. C. Y. Chang, A. Pralle, E. Y. Isacoff and C. J. Chang, *J. Am. Chem. Soc.*, 2004, **126**, 15392-15393.
6. S. Chen, R. Yuan, Y. Chai, L. Zhang, N. Wang and X. Li, *Biosens. Bioelectron.*, 2007, **22**, 1268-1274.
7. R. C. Matos, E. O. Coelho, C. F. Souza, F. A. Guedes and M. A. Matos, *Talanta*, 2006, **69**, 1208-1214.
8. Z. Wang, F. Liu, X. Teng, C. Zhao and C. Lu, *Analyst*, 2011, **136**, 4986-4990.
9. W. Chen, S. Cai, Q. Q. Ren, W. Wen and Y. D. Zhao, *Analyst*, 2012, **137**, 49-58.
10. M. Roushani, E. Karami, A. Salimi, and R. Sahraei, *Electrochim. Acta*, 2013, **113**, 134-140.
11. X. Y. Li, X. H. Liu, W. W. Wang, L. Li, and X. Q. Lu, *Biosens. Bioelectron.*, 2014, **59**, 221-226.
12. B. C. Dickinson, C. Huynh and C. J. Chang, *J. Am. Chem. Soc.*, 2010, **132**, 5906-5915.
13. G. Bartosz, *Clin. Chim. Acta.*, 2006, **368**, 53-76.
14. C. Amatore, S. Arbault, M. Guille and F. Lemaitre, *Chem. Rev.*, 2008, **108**, 2585-2621.
15. W. B. Nuwall and W. G. Ktihr, *Electroanalysis*, 1997, **9**, 102-109.
16. J. B. Jia, B. Q. Wang, A. G. Wu, G. J. Cheng, Z. Li, and S. J. Dong, *Anal. Chem.*, 2002, **74**, 2217-2223.
17. Y. P. Luo, H. Q. Liu, Q. Rui, and Y. Tian, *Anal. Chem.*, 2009, **81**, 3035-3041.
18. W. Lu, F. Liao, Y. Luo, G. Chang and X. Sun, *Electrochim. Acta*, 2011, **56**, 2295-2298.
19. X. Cao, Z. Zeng, W. Shi, P. Yep, Q. Yan and H. Zhang, *Small*, 2013, **9**, 1703-1707.
20. J. Tkac and T. Ruzgas, *Electrochem. Commun.*, 2006, **8**, 899-903.
21. B. Sýljukic, C. E. Banks, and R. G. Compton, *Nano Lett.*, 2006, **6**, 1556-1558.
22. C. X. Guo, X. T. Zheng, Z. S. Lu, X. W. Lou and C. M. Li, *Adv. Mater.*, 2010, **22**, 5164-5167.
23. P. Wu, Z. W. Cai, Y. Gao, H. Zhang and C. X. Cai, *Chem. Commun.*, 2011, **47**, 11327-11329.
24. T. Wang, H. Zhu, J. Zhuo, Z. Zhu, P. Papakonstantinou, G. Lubarsky, J. Lin and M. Li, *Anal. Chem.*, 2013, **85**, 10289-10295.
25. X. Sun, S. Guo, Y. Liu and S. Sun, *Nano Lett.*, 2012, **12**, 4859-4863.
26. Y. Zhang, C. Wu, X. Zhou, X. Wu, Y. Yang, H. Wu, S. Guo and J. Zhang, *Nanoscale*, 2013, **5**, 1816-1819.
27. S. Arbault, P. Pantano, J. A. Jankowski, M. Vuillaume, and C. Amatore, *Anal. Chem.*, 1995, **67**, 3382-3390.
28. F. Ai, H. Chen, S. H. Zhang, S. Y. Liu, F. Wei, X. Y. Dong, J. K. Cheng, and W. H. Huang, *Anal. Chem.*, 2009, **81**, 8453-8458.
29. X. Li, X. Liu, W. Wang, L. Li and X. Lu, *Biosens. Bioelectron.*, 2014, **59**, 221-226.
30. F. Xu, Y. Sun, Y. Zhang, Y. Shi, Z. Wen and Z. Li, *Electrochem. Commun.*, 2011, **13**, 1131-1134.
31. M. Sudan Saha, R. Li, M. Cai and X. Sun, *Electrochem. Solid-State Lett.*, 2007, **10**, B130-B133.
32. C. Li, J. Hu, T. Liu and S. Liu, *Macromolecules*, 2011, **44**, 429-431.
33. S. R. Gowda, A. L. M. Reddy, X. B. Zhan, H. R. Jafry and P. M. Ajayan, *Nano Lett.*, 2012, **12**, 1198-1202.
34. F. Léonard and A. A. Talin, *Nat. Nanotech.*, 2011, **6**, 773-783.
35. X. Y. Lang, H. Y. Fu, C. Hou, G. F. Han, P. Yang, Y. B. Liu and Q. Jiang, *Nat. Commun.*, 2013, **4**, 2169, DOI: 10.1038/ncomms3169.
36. C. F. Yu, F. L. Jia, Z. H. Ai and L. Z. Zhang, *Chem. Mater.*, 2007, **19**, 6065-6067.
37. J. H. Jiang and X. Y. Wang, *Electrochem. Commun.*, 2012, **20**, 157-159.
38. J. H. Jiang and X. Y. Wang, *ECS Electrochem. Lett.*, 2012, **1** (5), H21-H23.
39. J. T. Liu, L. S. Hu, Y. L. Liu, R. S. Chen, Z. Cheng, S. J. Chen, C. Amatore, W. H. Huang and K. F. Huo, *Angew. Chem. Int. Edit.*, 2014, **53**, 2643-2647.

ARTICLE

Journal Name

1 40. A. W. Griffith and J. M. Cooper, *Anal. Chem.* 1998, **70**, 2607-2612.

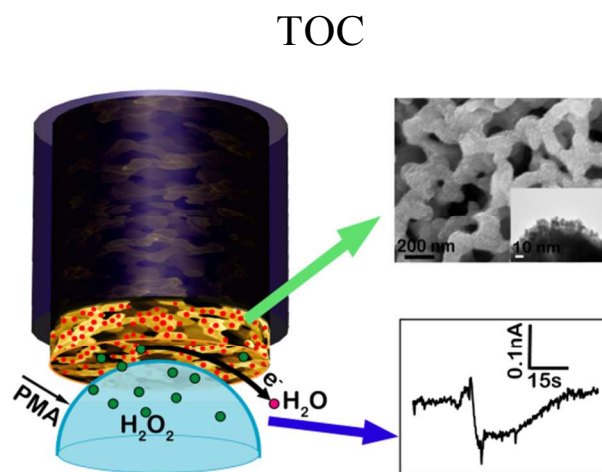
43. Z. M. Peng and H. Yang, *Nano Today*, 2009, **4**, 143–164.

2 41. P. Wu, Y. Qian, P. Du, H. Zhang and C. Cai, *J. Mater. Chem.*, 2012, **22**,
3 6402-6412.

44. Z. Chen, M. Waje, W. Li and Y. S. Yan, *Angew. Chem. Int. Ed.*, 2007,
4 **46**, 4060–4063.

5 42. S. Trasatti and O. A. Petrii, *Pure & Appl. Chem.*, 1991, **63**, 711-734.

Analyst Accepted Manuscript



We present a self-supported nanoporous gold/PtNPs microelectrode with a sub-nanomolar sensitivity to detect H_2O_2 release from single cells.